Soft-X-Ray–Induced Core-Level Photoemission as a Probe of Hot-Electron Dynamics in SiO_2

F. R. McFeely, E. Cartier, L. J. Terminello, A. Santoni,[a] and M. V. Fischetti
IBM Research Division, Thomas J. Watson Research Center, P.O. Box 218, Yorktown Heights, New York 10598
(Received 19 July 1990)

The line shape of the bulk Si $2p$ core-level photoemission peak is found to be strongly dependent on the thickness of SiO_2 overlayers through which the electrons are transmitted. This effect is strongly energy dependent. We demonstrate that it arises from strong energy-dependent carrier relaxation in SiO_2, and show how the effect may be used, in conjunction with Monte Carlo simulations, to extract energy-dependent scattering rates for electron-phonon and electron-electron scattering.

PACS numbers: 72.20.Dp, 72.80.Ng, 79.60.Eq

The understanding of hot-electron transport in SiO_2 has improved dramatically over the past decade. Major contributions to these advances have come from high-field electron-transport experiments through SiO_2 thin films in metal-oxide-semiconductor devices.[1-6] These studies demonstrated that substantial electron heating occurs at fields as low as 2 MV/cm,[1,2] and that with the highest sustainable fields in state-of-the-art films the majority of the electrons are stabilized with energies on the order of 4–6 eV.[3-6] This stabilization makes it inherently difficult to study the dynamics of carriers with energies much in excess of 6 eV by high-field transport techniques. It is clear, however, that velocity runaway by unstabilized electrons to above-band-gap kinetic energies, where electronic excitations become possible, is controlled by electron-energy-loss dynamics at energies greater than 6 eV.[7] Since these are the electrons which are responsible for impact ionization and carrier multiplication, an *a priori* understanding of critical fields for electron avalanche formation depends critically upon a detailed knowledge of the transport properties at the band-gap energy and above. In this Letter, we demonstrate the use of a new experimental approach, soft-x-ray core-level photoemission, which is uniquely suited for the study of electron-energy-loss dynamics in this heretofore inaccessible energy regime.

At sub-band-gap kinetic energies, Fischetti and coworkers[6,8,9] have developed a Monte Carlo scattering scheme which yields results in good agreement with internal photoemission measurements of scattering lengths[10] and successfully accounts for the stabilization of the bulk of the electron energy distribution in SiO_2 at 4–6 eV. These results indicated that acoustic-phonon scattering and its amplification of the effect of optical-phonon emission is the key to the stabilization process.[6] The acoustic-phonon scattering greatly increased the effective path length in the oxide, allowing for efficient loss of energy via the emission of energetic longitudinal-optical (LO) phonons. Without strong acoustic scattering, the LO-phonon scattering was too weak to cool the electrons sufficiently.

This model predicts that this stabilization mechanism should become increasingly effective with increasing energy. The acoustic scattering rate scales with the $\frac{3}{2}$ power of the electron kinetic energy, while optical-phonon scattering dies off only as $E_{\rm kin}^{-1/2}$, resulting in ever more effective carrier cooling. As will be shown below, however, our results are consistent with the above model of the scattering only at energies $E_{\rm kin} \leq 8$ eV. Above the band gap, our experiments demonstrate unambiguously that the acoustic scattering becomes steadily less important, and gradually dies away over the energy range of 8–18 eV. Modeling of the carrier relaxation in the high-energy regime is not as yet well established, and the various proposed schemes for SiO_2 differ considerably.[6-9,11,12] These differences arise partly from uncertainties concerning the SiO_2 conduction-band structure,[9,11] but, more fundamentally, there is no agreement concerning the theoretical treatment of acoustic-phonon scattering in the high-energy limit.[9,11,12] This scattering depends on the unknown short-wavelength (high-q) behavior of the ionic potential and the adiabatic approximation may fail.[13] Our data therefore provide an ideal basis for the critical evaluation of high-energy electron-phonon interaction theories. The data furthermore allow the determination of the energy dependence of electron-hole pair-production cross sections.

The experiments use the sharp Si $2p_{3/2}$ core-level photoemission peak arising from a Si(111) substrate as an internal source for zero-field electron transmission experiments through successively thicker overlayers of SiO_2. The information on the scattering process is extracted from the overlayer-induced changes in the substrate core-level intensity *and* line shape. By varying the photon energy, the probe electrons may be injected into the SiO_2 at any desired energy.

Samples were prepared by repetitive *in situ* oxidation of a clean Si(111) substrate. Oxidation temperatures varied between 750 and 900 °C, and oxygen pressures ranged from 10^{-5} to 0.2 Torr. In each case the sample was cooled to room temperature in the oxygen ambient to avoid pinhole formation. Following each oxidation, Si $2p$ core-level spectra were measured using constant-final-state (CFS) photoemission spectroscopy. In this method,[14] the electron-energy-analyzer kinetic energy is fixed, and the photon energy is swept to generate the

photoemission spectrum. The electron analyzer was an angle-integrating display instrument, and the photons were provided by the vacuum-ultraviolet ring of the National Synchrotron Light Source. Photoemission spectra of the Si $2p$ core-level region were collected at 2-eV intervals between 8 and 18 eV, and also at 30 eV. The latter spectra were used to determine the thickness of the films, by means of a measurement of the Si $2p$ emission intensity ratio between bulk substrate Si and the chemically shifted peak in the SiO_2 overlayer, in conjunction with published escape-depth and cross-section data.[15]

Typical spectra are shown in Fig. 1, which shows the substrate Si $2p$ core-level spectra measured at 8 eV (with respect to the SiO_2 conduction-band minimum) after transport through three different oxide overlayer thicknesses. The top panel shows a typical sharp spectrum characteristic of a thin overlayer. The Si $2p_{3/2}$ and $2p_{1/2}$ peaks are well described by Gaussian-broadened Lorentzian functions with a full width at half maximum of 410 meV. In passing to the 14.6- and 20.3-Å oxide overlayers, Figs. 1(b) and 1(c), these sharp features are drastically and asymmetrically broadened. The leading edge of the spectrum is much less sharp and the maxima shift to successively higher photon energies, the direction corresponding to energy loss. We shall demonstrate below that these drastic changes can be fully accounted for by carrier relaxation in the SiO_2 overlayer.

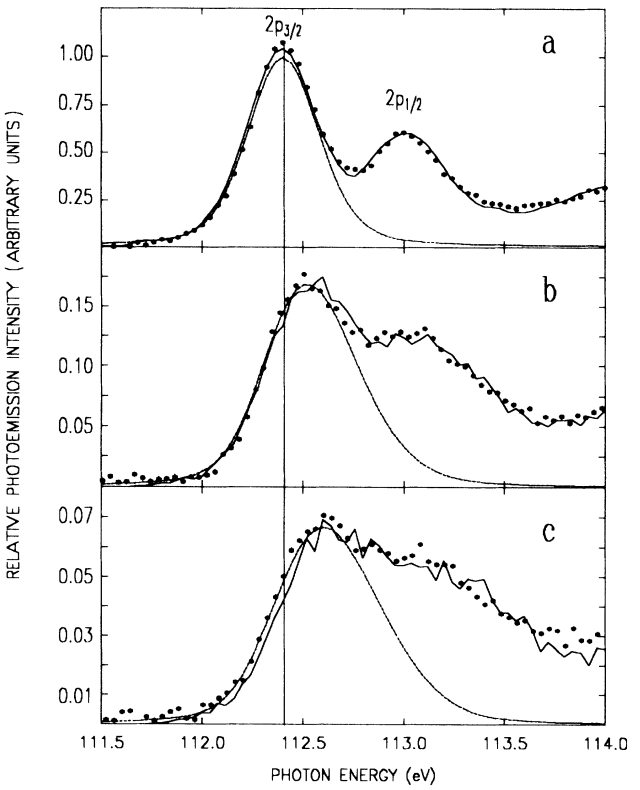

FIG. 1. The points show CFS photoemission spectra of the bulk Si $2p_{3/2}$ core level measured at 8 eV kinetic energy after transport through (a) 4.9-Å, (b) 14.6-Å, and (c) 20.3-Å SiO_2. A smooth background has been subtracted. The dashed lines give the Si $2p_{3/2}$ components derived from least-squares fits. The solid lines in (b) and (c) give the results of Monte Carlo simulations, using the energy distribution of (a) as input. Note that the intensities of the simulations are *not* scaled to match the data.

To present data from a large number of thicknesses obtained at a number of energies in a succinct manner, we have used peak fitting methods to extract the width and intensity of the Si $2p_{3/2}$ peaks. These two parameters are used to characterize the effect of the carrier relaxation accompanying transport through the oxide overlayers. These decompositions are shown by the dashed lines under the $2p_{3/2}$ peaks in the spectra of Fig. 1. Because of the asymmetry of the broadening, a special line shape must be employed to fit the thick-overlayer spectra accurately. This has been discussed at length in Ref. 14. Briefly, the line is described as a Poisson distribution of lines separated by 153 meV, the LO-phonon energy, with the individual components within the distribution constrained to have the same Gaussian-broadened Lorentzian shape and linewidth as the sharp, symmetric spectra measured for the thinnest overlayer (4.9 Å) studied.

In Fig. 2 we show the evolution of the bulk Si $2p_{3/2}$ linewidth, obtained by the method above, as a function of overlayer thickness for energies between 8 and 30 eV. The linewidth increases systematically with oxide overlayer thickness and decreases systematically with increasing kinetic energy. At 30 eV (bottom curve), the spectra actually sharpen slightly with increasing oxide thickness. This observation demonstrates conclusively that none of the observed broadening at lower energies is

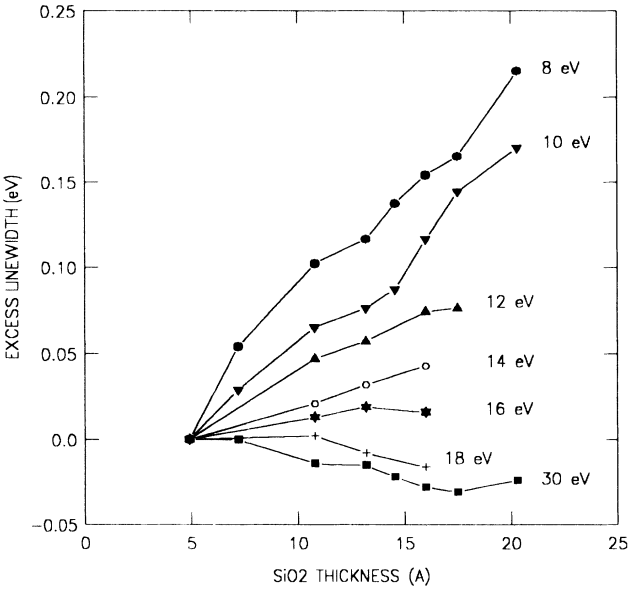

FIG. 2. The evolution of the Si $2p_{3/2}$ linewidth as a function of overlayer thickness, for the energies measured.

due to chemical or structural degradation of the underlying Si(111) substrate. Were such degradation in the underlying substrate occurring, it would be most severe in the vicinity of the Si/SiO_2 interface. The 30-eV spectra are, owing to the short escape depth from Si at this energy, the spectra most sensitive to the interfacial region. The fact that these spectra sharpen is evidence that the interfacial region is actually improving. This is most likely due to the better annealing afforded by the higher temperatures at which the thicker oxide samples were prepared.

The great utility of the data illustrated in Fig. 1 is that they may be used in conjunction with Monte Carlo simulations to derive the rates of acoustic-phonon scattering and electron-electron scattering directly. To show this we have employed a classical Monte Carlo simulation program which is essentially that of Refs. 6–8, modified to simulate the acquisition of the CFS spectra and to include the electron-electron scattering necessary at high energies. The phonon scattering, including both absorption and emission, is treated via a Fröhlich Hamiltonian (LO modes), the Harrison approximation [transverse-optical (TO) modes], and the deformation-potential approximation (acoustic modes) which further assumes umklapp-dominated isotropic scattering.

Of the three scattering modes entering the calculation, the LO-phonon scattering is well understood, and the parameters upon which its scattering matrix elements depend are accurately known. The Harrison potential for TO-phonon scattering is not so well known but even at upper-limit values set by low-energy photoemission data its effect is negligible.[16] The deformation potential for SiO_2, however, is poorly known, with estimates ranging from 2.5 to 5.0 eV. We have therefore chosen to regard it as an adjustable parameter. In order to reproduce the experimental observations, inelastic electron-electron scattering must also be included. We have also treated this scattering rate as a free parameter. Since the minimum energy loss possible in such a scattering event is on the order of the band-gap energy, a single scattering completely removes the electron from the spectrum and its further propagation need no longer be considered.

Returning to Fig. 1, the solid lines show the results of such a Monte Carlo simulation for a deformation potential of 3.3 eV and an electron-electron scattering rate of 3×10^{14} sec^{-1} at 8 eV kinetic energy. The solid curve of Fig. 1(a) was used as the input distribution and the injection into the additional oxide was assumed isotropic. The use of this thin oxide as a starting point eliminates any complications resulting from chemical inhomogeneities or potential discontinuities at the Si/SiO_2 interface. As can be seen, the simulation does a remarkably good job of reproducing the evolution of the line shape, intensity, and leading edge energy shift of the spectra. [There is *no* adjustment between simulation and experiment in Figs. 1(b) and 1(c) in either energy or intensity.] This is furthermore accomplished with a deformation potential well within the range of accepted values.[6,8]

The full sensitivity of the acoustic-phonon and electronic scattering rates to the data is illustrated in Fig. 3. For a given kinetic energy, each spectrum can be characterized by three parameters, the oxide overlayer thickness, the intensity of the Si $2p_{3/2}$ peak, and the excess $2p_{3/2}$ linewidth. In Fig. 3 we plot the 8-eV data and compare it to the results of the simulations in two planes of this three-dimensional parameter space, intensity versus excess linewidth (top) and intensity versus oxide thickness (bottom). The simulated spectra have been analyzed exactly as described above for the experimental data. In each panel, the experimental data (circles) and the values derived from the Monte Carlo simulations with optimum scattering rates (squares) are displayed. An important feature is illustrated for the 14.6-Å point, namely, that the simulations allow us to determine both the acoustic-phonon and the electron-electron scattering rates independently, not merely their sum. This is be-

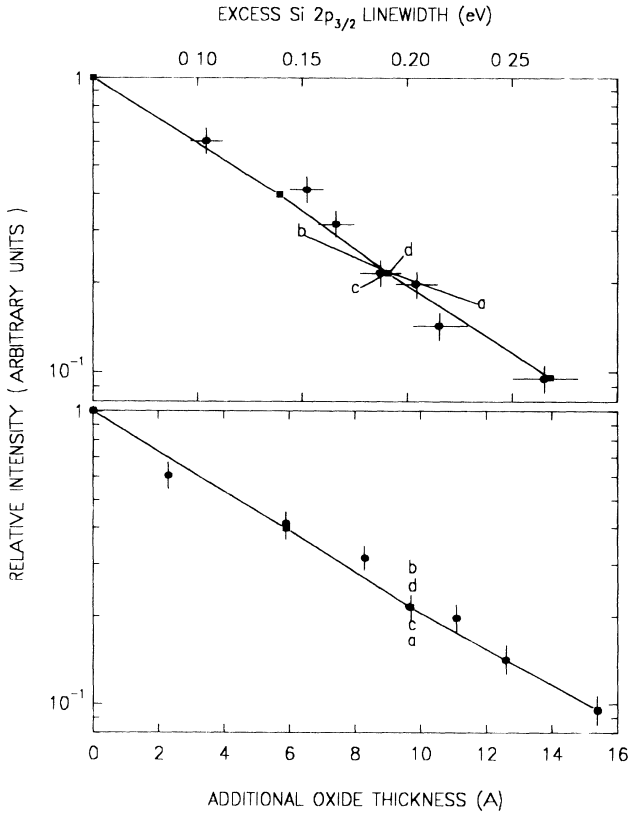

FIG. 3. Top panel: Si $2p_{3/2}$ relative intensity vs excess linewidth. Bottom panel: relative intensity vs overlayer thickness. The thinnest-oxide spectrum is taken as the unit of intensity, and the zero of extra thickness and excess linewidth. The circles are the experimental results for 8-eV electrons. The squares are the results of the Monte Carlo simulations, and are connected as an aid to the eye. The points represented by the labels *a*, *b*, *c*, and *d* show the results of 20% excursions from the best-fit values for the acoustic deformation potential and the electronic scattering rates.

cause effects of the two rates on a point in the broadening-intensity plane are largely uncoupled. This can be seen clearly from the points represented by the labels *a*, *b*, *c*, and *d*. Points *a* and *b* show the parameters resulting from a simulation with a $\pm 20\%$ change in the deformation potential maintaining the optimum electron-electron scattering rate of 3×10^{14} $\sec^{-1}$. Points *c* and *d* are the result for a $\pm 20\%$ excursion of the inelastic electron scattering rate at a constant deformation potential of 3.3 eV.

In conclusion, we have shown that high-resolution soft-x-ray core-level spectroscopy can serve as a sensitive zero-field probe of hot-electron dynamics. It is furthermore uniquely suited to the investigation of above-band-gap kinetic energies, where device-based methods are difficult to perform or interpret, and which is poorly understood at the present time. The 8-eV data were successfully analyzed above using the standard theoretical model. A glance at Fig. 2 will suffice to show that this cannot continue to hold true at higher kinetic energies. For a constant deformation potential, the acoustic-phonon scattering rate is predicted to increase between 8 and 18 eV.[8] This would cause the phonon broadening to increase with increasing energy, while the opposite trend is observed. Our data clearly show that the effect of acoustic-phonon scattering gradually dies away from 8 to 18 eV. The resolution of this conflict likely lies either in the failure of the assumed single-band density of states or in the transformation of the acoustic scattering from isotropic to a more atomiclike forward-peaked scattering. Previous workers have estimated that the critical energy for such a transition would occur at approximately 25 eV;[9] however, our data indicate that this process may be occurring at much lower energies. As mentioned above, there is no first-principles theory available at this time to model this process. A detailed semiempirical analysis of the evolution of the data to higher energies is currently in progress.

It is a pleasure to thank D. J. DiMaria for many fruitful discussions. A.S. gratefully acknowledges receipt of a Max Planck Gesellschaft Otto Hahn fellowship.

[a]Permanent address: ENEA-TIB c/o Sincrotrone Trieste, Padriciano 99, 34012 Trieste, Italy.

[1]D. J. DiMaria, M. V. Fischetti, E. Tierney, and S. D. Brown, Phys. Rev. Lett. **56**, 1284 (1984).

[2]D. J. DiMaria, M. V. Fischetti, M. Arienzo, and E. Tierney, J. Appl. Phys. **60**, 1719 (1986).

[3]T. N. Theis, D. J. DiMaria, J. R. Kirtley, and D. W. Dong, Phys. Rev. Lett. **52**, 1445 (1984).

[4]D. J. DiMaria, T. N. Theis, J. R. Kirtley, F. L. Pesavento, D. W. Dong, and S. D. Brorson, J. Appl. Phys. **57**, 1214 (1985).

[5]S. D. Brorson, D. J. DiMaria, M. V. Fischetti, F. L. Pesavento, P. M. Solomon, and D. W. Dong, J. Appl. Phys. **58**, 1302 (1985).

[6]M. V. Fischetti, D. J. DiMaria, S. D. Brorson, T. N. Theis, and J. R. Kirtley, Phys. Rev. B **31**, 8124 (1985).

[7]D. K. Ferry, in *The Physics and Technology of Amorphous SiO_2*, edited by Roderick A. B. Devine (Plenum, New York, 1988), p. 365.

[8]M. V. Fischetti, Phys. Rev. Lett. **63**, 1755 (1984).

[9]M. V. Fischetti and D. J. DiMaria, Phys. Rev. Lett. **55**, 2475 (1985).

[10]E. Cartier and P. Pfluger, Phys. Scr. **T23**, 235 (1988).

[11]W. Porod and D. K. Ferry, Phys. Rev. Lett. **54**, 1189 (1985).

[12]S. I. Zakharov and Yu. D. Fiveisky, Solid State Commun. **66**, 1251 (1988).

[13]J. M. Ziman, *Electrons and Phonons* (Oxford Univ. Press, Oxford, 1974).

[14]F. R. McFeely, E. Cartier, J. A. Yarmoff, and S. A. Joyce, Phys. Rev. B **42**, 5191 (1990).

[15]F. J. Himpsel, F. R. McFeely, A. Taleb-Ibrahimi, J. A. Yarmoff, and G. Hollinger, Phys. Rev. B **38**, 6084 (1988).

[16]E. Cartier (unpublished).